Phase-slip lines as a resistance mechanism in transition-edge sensors

Douglas A. Bennett, Daniel R. Schmidt, Daniel S. Swetz, and Joel N. Ullom

Citation: Applied Physics Letters **104**, 042602 (2014); doi: 10.1063/1.4863664
View online: http://dx.doi.org/10.1063/1.4863664
View Table of Contents: http://scitation.aip.org/content/aip/journal/apl/104/4?ver=pdfcov
Published by the AIP Publishing

Phase-slip lines as a resistance mechanism in transition-edge sensors

Douglas A. Bennett,[a] Daniel R. Schmidt,[b] Daniel S. Swetz, and Joel N. Ullom
National Institute of Standards and Technology, Boulder, Colorado 80305, USA

(Received 4 October 2013; accepted 14 January 2014; published online 31 January 2014)

The fundamental mechanism of resistance in voltage-biased superconducting films is poorly understood despite its importance as the basis of transition-edge sensors (TESs). TESs are utilized in state-of-the-art microbolometers and microcalorimeters covering a wide range of energies and applications. We present a model for the resistance of a TES based on phase-slip lines (PSLs) and compare the model to data. One of the model's predictions, discrete changes in the number of PSLs, is a possible explanation for the observed switching between discrete current states in localized regions of bias. [http://dx.doi.org/10.1063/1.4863664]

Just as the onset of resistance in current-carrying superconducting films remains a topic of active study,[1,2] so too are there unanswered questions concerning the evolution of dissipation from small but finite levels to the full, normal-state resistance. The superconducting transition is difficult to study in biased devices since they are prone to thermal runaway in the resistive state. The complications due to thermal runaway can be avoided by taking advantage of the negative electrothermal feedback (ETF) that is a feature of transition-edge sensors (TESs).[3] A TES is a superconducting film with a weak thermal link to the bath with the film maintained in the superconducting transition by using a voltage bias. A TES acts as a very sensitive thermometer since small changes in temperature can cause large changes in resistance. Microbolometers and microcalorimeters based on TESs are in use in a large range of applications including an independent confirmation of the existence of dark energy using only the cosmic microwave background[4] and the search for weakly interacting massive particles (WIMPs).[5] The increasing prominence of TESs as tools for fundamental science is strong motivation to better understand the physical mechanism underlying resistance in these devices. However, a physical model for the resistance of TESs that capture the dependence of resistance on both temperature and current has been elusive.

A description of TES resistance based on the resistively shunted junction (RSJ) model proposed by Kozorezov *et al.*[6] was motivated by observations of Sadleir *et al.*[7] suggestive of very long coherence lengths in some TESs. Alternatively, Bennett *et al.*[8] showed that a phenomenological model, based on the idea of parallel "fluids" consisting of the normal and super currents, was able to describe much of the general behavior of larger TESs, including local regions of the current-voltage (IV) curves and the partial derivatives of resistance with respect to temperature and current.

Analysis of the partial derivative of resistance with respect to current at constant temperature (β_I) suggests that the RSJ model is applicable to smaller devices where the length of the device is on the order of a few times the superconducting coherence length (ξ), while the two-fluid model is applicable to larger devices.[9] However, neither model predicts the discrete regions of the transition that have been recently reported to show evidence of switching between distinct current states.[10,11] These regions also show increased noise that, along with related observations of kinks in a TES's transient response to deposited energy, can degrade detector performance and make energy calibration more difficult. In this Letter, we describe a model of the resistance in TESs based on phase-slip lines (PSLs), compare it to data, and show how this model can explain the observation of multiple current states.

One of the physical motivations for describing the TES resistance with a two-fluid model[12] was the model for the voltage drop across phase-slips in superconducting filaments proposed by Skocpol-Beasley-Tinkham (SBT).[13] Many groups have observed that a superconducting filament or nanowire that exceeds its critical current (I_c) does not jump directly from the superconducting state to the normal state as is predicted by the Ginzburg-Landau theory (G-L). Instead, the IV curve shows a series of regular voltage steps as current increases.[14] The first onset of voltage follows the G-L prediction and defines the I_c of the device. Between steps, the differential resistance is an integer multiple of the resistance after the first jump. This behavior is attributed to phase-slips, where the phase of the superconducting order parameter is increasing at different rates on the two sides of a spatially localized region.

The phase-slip process is fundamentally cyclic where the local super-current (I_s) is oscillating in time.[14] At a bias current above the local critical current (I_c), a zero-voltage superconducting state is no longer possible and an electric field appears in this region. The electric field accelerates Cooper pairs until I_s is above I_c, resulting in a collapse of the order parameter. The total current (I) remains constant throughout the process. Therefore, all the current is briefly carried by the normal current as quasiparticles, which in turn allows I_s to be reestablished and the cycle repeats. Averaged over time, the I_s in the phase-slip region is some fraction of the total critical current $\overline{I_s} = c_I I_c$. The remainder of the current, $I - \overline{I_s}$, is carried by the quasiparticles. The length scale on either side of the phase-slip, where the current is carried by the quasiparticles, is Λ_{Q^*}. Λ_{Q^*} has been shown to have a weak temperature dependence $\Lambda_{Q^*}(T) \approx \Lambda_{Q^*}(0)/(1 - T/T_c)^{1/4}$,[15,16] where T_c is the critical temperature. One-dimensional phase

[a]Also at University of Denver, Denver, Colorado 80208, USA. Electronic mail: Douglas.Bennett@nist.gov.
[b]Also at University of Colorado, Boulder, Colorado 80309, USA.

slips, known as phase-slip centers (PSCs), have been extensively studied in whiskers, micro-bridges, and most recently in nanowires, i.e., in relation to quantum phase-slips.[17]

In the SBT model, the voltage across an isolated PSC is given by $V = 2\Lambda_{Q^*} R_n (I - c_I I_c)/L$, where L is the length of the device and R_n is the normal resistance of the device. The SBT model is sufficient to describe most of the properties of an isolated PSC. The SBT model has the same functional form as the two-fluid model, which was compared to measured data for TESs in Ref. 8. In this comparison, fixed empirical coefficients were used in place of the physical parameters of the SBT model. Since the two-fluid coefficients were fixed, the two-fluid model in Ref. 8 describes only a small portion of the transition. The SBT model gives a physical basis to the two-fluid parameters across the whole transition and enables comparison to data without empirical coefficients.

Numerous studies of current-biased superconducting 2D films[18–21] have shown step-like structure similar to PSCs in one-dimensional devices. The steps were associated with PSLs, the exact 2D analogue to PSCs except that the order parameter may vary across the film perpendicular to the current flow.[22]

The planar dimensions of the films used in this study greatly exceed the coherence length so PSLs are a candidate resistance mechanism. Since the normal resistance in a 2D film is typically low compared to the 1D case, current-biased 2D films are prone to thermal runaway where the thermal conductance of the film or substrate cannot remove the heat created by the Joule heating of the film in the dissipative state.[18] However, the problem of over-heating is solved in TESs by the negative ETF provided by the voltage bias due to a small shunt resistor connected in parallel.[3] Therefore, TESs operate in a unique parameter space where the highest currents are encountered at low resistance fractions and where ETF allows higher resistance fractions to be sampled where larger numbers of phase-slips may be present. As a result, TESs provide an attractive system in which to explore the interacting phase-slip regime.

The SBT model was extended by Tinkham[23] using the same assumptions as in Ref. 13 to explicitly describe the case of multiple interacting PSCs. Here, we adapt Tinkham's result to voltage-biased, two-dimensional films. As will be shown shortly, the resulting model is strikingly successful at explaining both local and large-scale structure in $R(I,T)$ data from TESs. The voltage drop across n_{ps} equally spaced phase-slips in a channel of length L is

$$V_n = \frac{2n_{ps}\Lambda_{Q^*}}{L} R_n (I - c_I I_c) \tanh\left(\frac{L}{2n\Lambda_{Q^*}}\right). \quad (1)$$

Ref. 23 also describes the criteria for determining the number of phase-slips at a given bias current in an ideal superconductor ignoring the leads. The argument is basically that for a given number of phase-slips (n_{ps}), once I_s at any point exceeds I_c, a new phase-slip is formed. Since $\overline{I_n}$ is decaying exponentially moving away from a phase-slip, $\overline{I_s}$ is largest midway between two phase-slips. Assuming equally spaced phase-slips, the maximum current for n_{ps} is

$$I_{max,n} = I_c \frac{\cosh[L/(2(n_{ps}+1)\Lambda_{Q^*})] - c_I}{\cosh[L/(2(n_{ps}+1)\Lambda_{Q^*})] - 1}. \quad (2)$$

Equations (1) and (2) are not fundamentally specific to 1D geometries so we will use them to describe PSLs in 2D films. We will first use this simple description of PSLs to create a model for the resistance of a TES, $R(T,I)$, and then compare this model to a TES similar to the devices targeted at gamma-ray spectroscopy applications described elsewhere.[24] In discussing the model, we will use the measured device parameters when available. The remaining free parameters will be identified appropriately.

Before modeling $R(T,I)$ for our TESs, the temperature dependence of I_c must be determined. For the device discussed in this letter, the temperature of the TES low in the transition is predicted to change by less than a percent of T_c. Over this temperature range, I_c is well described in our large devices by the G-L critical current $I_c(T) = I_{c0}(1 - T/T_c)^{3/2}$, where $I_{c0} = I_c\,(T = 0)$ and T_c is the temperature where I_c goes to zero as determined by fits to I_c as a function of T. In practice, since this temperature dependence is not valid well below T_c, I_{c0} is a fitting parameter that is determined by measurement.

Using Eqs. (1) and (2), we can calculate the IV characteristic at fixed temperatures. Figure 1(a) shows the IVs at five different fixed temperatures below $T_c = 102.83\,\text{mK}$ with $R_n = 10.2\,\text{m}\Omega$, $L = 400\,\mu\text{m}$, $\Lambda_{Q^*}(T = 0) = 3\,\mu\text{m}$, and $I_{c0} = 260\,\text{mA}$. The voltage jumps correspond to a change in

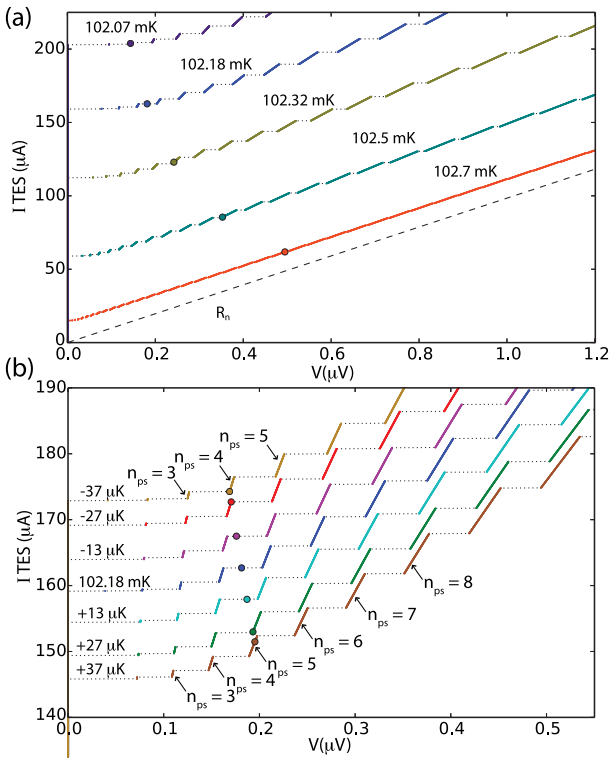

FIG. 1. (a) Solid lines are the calculated voltage across the TES using Eqs. (1) and (2) at five different temperatures. The corresponding dotted lines are to help guide the eye between resistive steps. The critical current at each temperature is determined by the G-L critical current with a $T_c = 102.83\,\text{mK}$ and $I_{c0} = 260\,\text{mA}$. The corresponding point for each fixed temperature is the equilibrium solution using Eqs. (3) and (4). (b) Same as (a) except for a narrow range of temperatures around 102.18 mK.

the n_{ps} when $I_{TES} > I_{max,n}$, and between voltage steps, the resistance is constant. As n_{ps} gets large, the resistance of the steps approaches R_n. Finally, each resistance step extrapolates back to $c_I I_c$ at $V = 0$. The strong dependence of I_c on T results in more steps with smaller voltage jumps as T approaches T_c.

To achieve an effective voltage bias of the TES, the superconducting film is placed in parallel with a shunt resistor R_s. The TES is biased by passing a current I_t through the parallel combination. I_t will divide between R_s and the TES such that the voltage drops are equal

$$(I_t - I)R_s = \frac{2n_{ps}\Lambda_{Q^*}}{L} R_n (I - c_I I_c(T)) \tanh\left(\frac{L}{2n_{ps}\Lambda_{Q^*}}\right). \quad (3)$$

The Joule heating due to power delivered to the TES from the source is IV. A TES has a weak thermal link to the bath, often consisting of a silicon-nitride membrane. The power flowing between the superconducting film at temperature T and the bath at temperature T_b has a power law dependence $P = k(T^n - T_b^n)$, where n is the thermal conductance exponent and the prefactor k is related to the thermal conductance G by $k = G/(nT^{n-1})$.[3] In thermal equilibrium, the Joule heating from TES current must be balanced by the heat leaving the TES through its thermal conductance

$$IV(I,R) = k(T^n - T_b^n). \quad (4)$$

Although the heating is localized at the PSLs,[25] the thermal conductance within the film is much larger than the thermal conductance to the bath, and therefore the film will have an approximately uniform temperature determined by the overall power balance. At a given I_t, Eqs. (3) and (4) can be solved to find T and I. Conversely, for a given T, we can solve for I and I_t. The points in Fig. 1(a) are the equilibrium solution at the fixed temperature of the corresponding IV assuming $T_b = 85$ mK, $n = 3.2$, $k = 9.80$ nW/K$^{3.2}$, and $R_s = 0.3$ mΩ.

At specific values of I_t or T, the simultaneous solution to Eqs. (3) and (4) occurs on a voltage step between n_{ps} and $(n+1)_{ps}$. This is demonstrated in Fig. 1(b), where the parameters are the same as the parameters in Fig. 1(a), except over a narrower range of fixed temperatures around $T = 102.18$ mK (blue line). For a temperature 27 μK warmer (green line), the equilibrium value (green circle) occurs when $n_{ps} = 5$. For a temperature 27 μK cooler (red line), the equilibrium value (red circle) occurs when $n_{ps} = 4$. However, in between these temperatures, the equilibrium solution falls on a voltage step. At $T = 102.18$ mK, the blue dot is the equilibrium value assuming an interpolation between the $n_{ps} = 4$ and $n_{ps} = 5$ states. However, a superconducting film can support only integer values of PSLs, and the dynamics of how the film switches states is an open question. Since the details of what happens on a voltage step are outside the scope of this Letter, we will take a simple approach and track both the n_{ps} and $(n+1)_{ps}$ when the solution to Eqs. (3) and (4) would otherwise fall on a voltage step.

Figure 2 shows the measured IV characteristic (blue points) of a representative TES that consists of a 400 μm by 400 μm MoCu film on a silicon-nitride membrane with normal-metal banks on the edges of the film parallel to

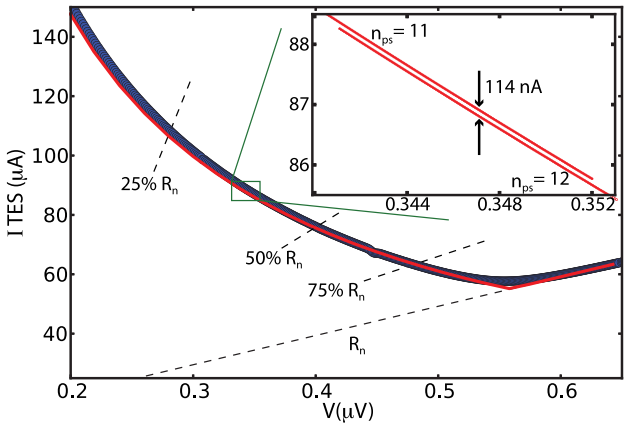

FIG. 2. (a) Blue circles are the measured IV characteristic at $T_b = 85$ mK. The red line is the equilibrium solution to Eqs. (3) and (4) for the measured TES parameters. The inset shows a region around 38% R_n in the region of the $n_{ps} = 12$ to $n_{ps} = 11$ transition.

current flow. While interdigitated normal-metal bars perpendicular to the direction of current flow are commonly used in TESs to reduce noise, they introduce spatial variation[26] that complicates comparison with any simple model and were omitted in this work. To measure the IV curve at a particular bath temperature, I_t is swept from a high value that drives the device normal down though the transition and into the superconducting state. I is measured using a SQUID ammeter and V is calculated from $I_t - I$ and the independently measured shunt resistance. The bias point is usually referenced by the resistance as a percentage of R_n. The IV was densely sampled in order to study local structure in the transition.

The red line in Fig. 2 is the solution to Eqs. (3) and (4) for the device parameters introduced previously. The model fits the data well across a wide range of the transition. The only parameters in this calculation that were not independently measured were c_I and $\Lambda_{Q^*}(0)$. $c_I = 0.55$ is in the range of observed values in the literature, i.e., $c_I = 0.3$ to 0.8 in Stuivinga *et al.*[25] The best fit for $\Lambda_{Q^*}(0)$ is 3 μm. This is consistent with $\Lambda_{Q^*}(0)$ between 3 μm and 6 μm determined from the distribution of currents in a TES.[26] The inset shows the prediction of the model around the voltage step corresponding to the change from $n_{ps} = 12$ to $n_{ps} = 11$. The current difference between the two states at a fixed voltage in the step region is 114 nA.

Figure 3 shows a contour plot around a bias of 38% R_n of the same IV as in Fig. 2. In this case, instead of averaging the measured I, the measured values were histogrammed to show the distribution of I for a given I_t. Below voltages of 0.342 μV and above 0.350 μV, there is a single current state. However, between these voltages, the current switches between two possible current states separated by ≈0.12 μA. The current difference between these states is consistent with the predictions of the model for the same TES parameters shown in the inset of Fig. 2 and suggests that the observed switching between distinct current states resulting in a bimodal current distribution[10,11] is caused by changes in the number of PSLs. This evidence, taken together with the excellent fits to the full IV curve, is strong evidence that PSLs are the underlying mechanism for resistance in TESs that are long enough that weak-link effects are minimal.

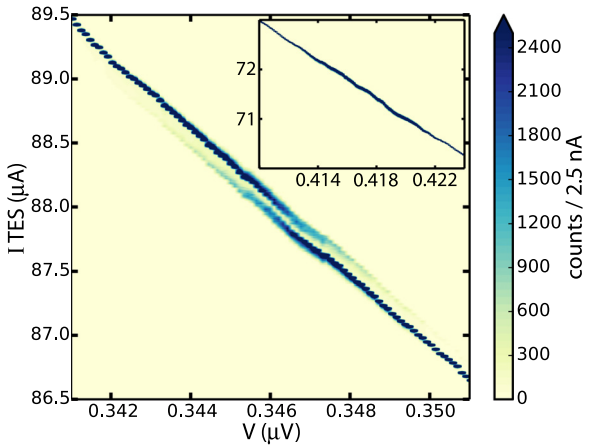

FIG. 3. The measured *IV* characteristic in the region of 38% R_n for $T_b = 85$ mK. At each bias voltage, 1 30 000 measurements of the current are histogrammed to show the distribution of currents. The inset shows the *IV* in the region of 57% R_n.

The model predicts that the number of PSLs varies widely across the transition. Hence, it is logical to ask how many of the predicted PSLs are observed. For reasons explained shortly, we divide the transition into four resistance regions: >60% R_n, 35%–60% R_n, 10%–35% R_n, and <10% R_n.

Both internal and external temperature fluctuations are capable of obscuring the distinct current states of the PSLs. For the device discussed in this Letter, and at an integration time necessary to obtain the statistics to resolve the difference between neighboring PSLs, the external temperature fluctuations dominate the internal fluctuations higher in the transition where the current difference between neighboring PSLs is small. In our measurement setup, fluctuations in the bath temperature are on the order 10 μK RMS. Above 60% R_n, the resulting fluctuations in device current are larger than the predicted separation in current between neighboring PSL states (<60 nA), obscuring the distinct current states. In fact, only one PSL feature is observed in this resistance range around 70% R_n. The size and shape of this feature are consistent with the near-simultaneous appearance of several PSLs, making this change observable while changes by one PSL are obscured.

Above 35% R_n and below 60% R_n where the PSL states are separated by more than the current noise, the model predicts five changes in the number of PSLs. In our data, we only observe switching between current states for two of the five possible steps. The second bimodal state, shown in the inset of Fig. 2, occurs at 57% R_n, near where the separation between states is similar to the current noise. Since the separation between the states is similar to the noise of the individual state, the distinct states are not observed and instead the overall distribution widens in the region of PSL compared to away from the PSL.

When the *IV* curve is sampled between 10% R_n and 35% R_n, there are specific bias points where the SQUID ammeter is unable to measure the TES current. At these points, the flux-locked loop used to linearize the output of the readout SQUID is unable to track the TES current. The current separation between states of different n_{ps} is predicted to be larger at low resistance values. Further, the PSL model predicts that the logarithmic derivative of resistance with respect to temperature at constant current (α_I) increases rapidly low in the transition. It also predicts even larger excursions in α_I at resistance values where the number of PSLs changes. In these high α_I regions, the TES is especially prone to electrothermal oscillations.[3] It is likely that increased electrothermal instability combined with the larger differences between the currents of neighboring PSLs states, 1 μA for $n_{ps} = 5$ to $n_{ps} = 4$, causes the flux-lock loop to fail. For the data shown in Fig. 2, we observe four bias points between 10% R_n and 35% R_n that are unstable for our SQUID readout and that we associate with changes in the number of PSLs. The PSL model predicts six such points over the same resistance range.

Below 10% R_n, our SQUID readout system is entirely unable to keep lock due to the effects outlined above, and we can draw no conclusions about the number of PSLs present. So, we can reasonably expect to be able to detect PSLs over the resistance range 10%–60% R_n, and we observe six of the eleven features predicted. The large number of detected PSL features strongly supports the idea that the normal-state resistance is achieved by increases in n_{ps}.

Why are all the predicted PSL features not observed? We note that Eq. (2) is based on a uniform film and ignores potential local defects and proximitization from the leads. PSLs will preferentially form around defects where the local order parameter is reduced, so that the assumption of evenly spaced PSLs is extremely idealized. Also, our model tells us only when the equilibrium solution is on a step, and not exactly when or how it changes between steps. Further work is needed to predict how changes in n_{ps} occur before firm conclusions can be drawn from the large but incomplete number of PSL features observed to date.

To summarize, the bi-stable currents observed in some regions of the *IV* curve of a TES are caused by changes in the number of PSLs in the superconducting film. Currently, the concept of PSLs provides the only physical model accounting for these features. These results are suggestive that, for TESs outside the weak-link regime, phase-slip lines are the mechanism for the observed resistance. Understanding the mechanism for resistance opens up the possibility of controlling the transition shape to meet the needs of emerging applications. Also, this model allows the resistance to be calculated across the entire transition, enabling the modeling of TES microcalorimeters beyond the small signal limit and the use of a model-based energy calibration. An important next step is to develop an understanding of the dynamics of the switching between states with different n_{ps}. A more complex model that includes information about the device geometry, possibly utilizing the time-dependent Ginzburg-Landau equations,[22] may be necessary to predict the exact position and density of the changes in n_{ps} in actual devices. Improved understanding of the conditions for phase-slips will enable the design of new detectors that are optimized to minimize or avoid the transitions between phase-slips and the associated noise and instability.

The authors acknowledge the support of the U.S. Department of Energy through the Office of Nonproliferation Research and Development and the Office of Nuclear Energy. Contribution of a U.S. government agency, not subject to copyright.

[1]M. Sahu, M.-H. Bae, A. Rogachev, D. Pekker, T.-C. Wei, N. Shah, P. M. Goldbart, and A. Bezryadin, Nat. Phys. **5**, 503 (2009).
[2]O. V. Astafiev, L. B. Ioffe, S. Kafanov, Y. A. Pashkin, K. Y. Arutyunov, D. Shahar, and O. Cohen, Nature **484**, 355 (2012).
[3]K. Irwin and G. Hilton, "Topics in applied physics," in *Cryogenic Particle Detection* (Springer-Verlag, 2005), Vol. 99, pp. 63–149.
[4]B. D. Sherwin, J. Dunkley, S. Das, J. W. Appel, J. R. Bond, C. S. Carvalho, M. J. Devlin, R. Dünner, T. Essinger-Hileman, J. W. Fowler *et al.*, Phys. Rev. Lett. **107**, 021302 (2011).
[5]The CDMS II Collaboration, Science **327**, 1619 (2010).
[6]A. Kozorezov, A. A. Golubov, D. D. E. Martin, P. A. J. de Korte, M. A. Lindeman, R. A. Hijmering, J. van der Kuur, H. F. C. Hoevers, L. Gottardi, M. Y. Kupriyanov, and J. K. Wigmore, Appl. Phys. Lett. **99**, 063503 (2011).
[7]J. E. Sadleir, S. J. Smith, S. R. Bandler, J. A. Chervenak, and J. R. Clem, Phys. Rev. Lett. **104**, 047003 (2010).
[8]D. Bennett, D. Swetz, R. Horansky, D. Schmidt, and J. Ullom, J. Low Temp. Phys. **167**, 102 (2012).
[9]D. A. Bennett, D. S. Swetz, D. R. Schmidt, and J. N. Ullom, Phys. Rev. B **87**, 020508 (2013).
[10]M. Croce, M. Bacrania, E. Bond, D. Dry, W. Moody, M. Rabin, D. Bennett, G. Hilton, R. Horansky, V. Kotsubo *et al.*, J. Low Temp. Phys. **167**, 955 (2012).
[11]V. Kotsubo, D. Bennett, M. Croce, M. Rabin, D. Schmidt, and J. Ullom, IEEE Trans. Appl. Supercond. **23**, 2100203 (2013).
[12]K. D. Irwin, G. C. Hilton, D. A. Wollman, and J. M. Martinis, J. Appl. Phys. **83**, 3978 (1998).
[13]W. Skocpol, M. Beasley, and M. Tinkham, J. Low Temp. Phys. **16**, 145 (1974).
[14]M. Tinkham, *Introduction to Superconductivity* (Dover Publications, Inc., 1996).
[15]A. Schmid and G. Schön, J. Low Temp. Phys. **20**, 207 (1975).
[16]A. Kadin, W. Skocpol, and M. Tinkham, J. Low Temp. Phys. **33**, 481 (1978).
[17]M.-H. Bae, R. Dinsmore III, M. Sahu, and A. Bezryadin, New J. Phys. **14**, 043014 (2012).
[18]E. Il'ichev, V. Kuznetsov, and V. Tulin, JETP Lett. **56**, 295 (1992).
[19]V. Dmitriev and I. Zolochevskii, Supercond. Sci. Technol. **19**, 342 (2006).
[20]E. Bezuglyi and I. Zolochevskii, Low Temp. Phys. **36**, 1008 (2010).
[21]I. Dmitrenko, Low Temp. Phys. **22**, 648 (1996).
[22]G. Berdiyorov, A. Elmurodov, F. Peeters, and D. Vodolazov, Phys. Rev. B **79**, 174506 (2009).
[23]M. Tinkham, J. Low Temp. Phys. **35**, 147 (1979).
[24]D. Bennett, R. Horansky, D. Schmidt, A. Hoover, R. Winkler, B. Alpert, J. Beall, W. Doriese, J. Fowler, C. Fitzgerald *et al.*, Rev. Sci. Instrum. **83**, 093113 (2012).
[25]M. Stuivinga, C. Ham, T. Klapwijk, and J. Mooij, J. Low Temp. Phys. **53**, 633 (1983).
[26]D. Swetz, D. Bennett, K. Irwin, D. Schmidt, and J. Ullom, Appl. Phys. Lett. **101**, 242603 (2012).